THE JOURNAL OF BIOLOGICAL CHEMISTRY
Vol. 279, No. 30, Issue of July 23, pp. 31374–31382, 2004
Printed in U.S.A.

Prefibrillar Amyloid Protein Aggregates Share Common Features of Cytotoxicity*

Received for publication, January 13, 2004, and in revised form, May 6, 2004
Published, JBC Papers in Press, May 6, 2004, DOI 10.1074/jbc.M400348200

Monica Bucciantini‡, Giulia Calloni‡, Fabrizio Chiti‡, Lucia Formigli§, Daniele Nosi§, Christopher M. Dobson¶‖, and Massimo Stefani‡‡‡**

*From the ‡Department of Biochemical Sciences, the **Center of Excellence for Molecular and Clinical Studies on Chronic, Inflammatory, Degenerative, and Tumoral Diseases for the Development of New Therapies, and the §Department of Anatomy, Histology and Forensic Medicine, University of Florence, 50134 Florence, Italy and the ¶Department of Chemistry, University of Cambridge, Cambridge CB2 1EW, United Kingdom*

The intracellular free Ca^{2+} concentration and redox status of murine fibroblasts exposed to prefibrillar aggregates of the HypF N-terminal domain have been investigated *in vitro* and *in vivo* using a range of fluorescent probes. Aggregate entrance into the cytoplasm is followed by an early rise of reactive oxygen species and free Ca^{2+} levels and eventually by cell death. Such changes correlate directly with the viability of the cells and are not observed when cell are cultured in the presence of reducing agents or in Ca^{2+}-free media. In addition, moderate cell stress following exposure to the aggregates was found to be fully reversible. The results show that the cytotoxicity of prefibrillar aggregates of HypF-N, a protein not associated with clinical disease, has the same fundamental origin as that produced by similar types of aggregates of proteins linked with specific amyloidoses. These findings suggest that misfolded proteinaceous aggregates stimulate generic cellular responses as a result of the exposure of regions of the structure (such as hydrophobic residues and the polypeptide main chain) that are buried in the normally folded proteins. They also support the idea that a higher number of degenerative pathologies than previously known might be considered as protein deposition diseases.

Approximately 20 different peptides or proteins, including the Aβ peptides, β_2-microglobulin, transthyretin, lysozyme, α-synuclein, and the prion protein, are the main components of amyloid aggregates *in vivo*, each being associated with a specific disease such as Alzheimer's, Parkinson's, and prion diseases, type 2 diabetes, and systemic amyloidoses. In these pathologies it is likely that the impairment of cellular function is a direct consequence of the interaction of cellular components with protein aggregates that may be present, in some cases, at very low levels (1, 2). In systemic non-neuropathic diseases, however, the accumulation in tissues and organs of large amounts of amyloid deposits may in itself be the primary origin of the clinical symptoms (2, 3). In some cases the proteins deposited are wild-type, as in sporadic amyloidoses, and in other cases they are modified by specific genetic mutations as in early onset familial diseases (4, 5).

Since 1998, an increasing number of natural or *de novo* designed sequences of proteins or peptides that are not associated with any known medical condition have been shown to aggregate *in vitro* into fibrils that are indistinguishable from those associated with the amyloid diseases (reviewed in Ref. 6). In the case of globular proteins, aggregation is found to require destabilizing conditions such that the proteins involved are at least partially unfolded but still able to form intramolecular interactions, notably those involving hydrogen bonding (7). These and other findings indicate that amyloid aggregation is a generic property of the polypeptide chain, most probably linked to the common structure of the peptide backbone (7–9). They also increase dramatically the number of proteins one can investigate to assess general features underlying protein misfolding and aggregation as well as the interaction of the aggregates with cells.

Recently, evidence is beginning to emerge suggesting that the effects of aggregation on cellular function might be very similar for different proteins. In particular, aggregates of two proteins unrelated to disease, the SH3[1] domain from the bovine phosphatidylinositol 3-kinase and the N-terminal domain of the *Escherichia coli* HypF (HypF-N) have been investigated from this perspective. Both of these proteins form amyloid fibrils under mild denaturing conditions (10, 11), and as observed for other amyloidogenic proteins, various prefibrillar aggregates are formed prior to the growth of mature fibrils, whose appearance often requires much longer periods of time (10, 11). Both proteins have been found to be toxic to cells only when added to the culture media in their prefibrillar state (12).

The findings on the cytotoxicity of the proteins that are not associated with disease are closely similar to the conclusions drawn from studies on disease-associated proteins such as the Aβ peptides, α-synuclein, and transthyretin (1, 13–17); these conclusions suggest that the cytotoxicity associated with aggregation may be determined by common features of specific types of aggregates rather than by specific amino acid sequences (12). The latter conclusion is also supported by recent findings providing evidence that the soluble prefibrillar aggregates of a range of different peptides and proteins are all recognized by polyclonal antibodies raised against a molecular mimic of soluble Aβ oligomers; the same antibodies fail to recognize the corresponding mature fibrillar aggregates, whereas they sup-

* This work was supported by grants from Italian MIUR Projects RBNE01S29H_004 and 2002058218-001. The costs of publication of this article were defrayed in part by the payment of page charges. This article must therefore be hereby marked "*advertisement*" in accordance with 18 U.S.C. Section 1734 solely to indicate this fact.

‖ Supported in part by a Programme Grant from the Wellcome Trust. To whom correspondence may be addressed: Dept. of Chemistry, Lensfield Road, Cambridge CB2 1EW, UK. E-mail: cmd44@cam.ac.uk.

‡‡ To whom correspondence may be addressed: Dept. of Biochemical Sciences, Viale Morgagni 50, 50134 Florence, Italy. E-mail: stefani@scibio.unifi.it.

[1] The abbreviations used are: SH, Src homology; HypF-N, HypF N-terminal domain; MTT, 3-(4,5-dimethylthiazol-2-yl)-2,5-diphenyltetrazolium bromide; PBS, phosphate-buffered saline; MOPS, 3-(*N*-morpholino)propanesulfonic acid; ROS, reactive oxygen species; CM-H_2 DCFA, 2′,7′-dihydrodichlorofluorescein diacetate; AM, acetoxymethylester.

press the cytotoxicity of the prefibrillar aggregates (18). These findings indicate that the prefibrillar aggregates of proteins and peptides that form amyloid fibrils share common structural features that differ from those displayed both by their nonaggregated precursors and by the mature fibrils; they also argue against specific mechanisms of toxicity of the differing amyloid aggregates. Therefore, an increasing body of evidence supports the idea that the ability to form amyloid aggregates and the toxicity of these aggregates are generic properties of peptides and proteins. It also suggests that, in general, the most highly cytotoxic aggregates are the early prefibrillar assemblies or, possibly in some cases, the individual misfolded molecules (19) rather than mature fibrils.

To explore in depth the fundamental origins of the cytotoxicity of early aggregates of proteins that ultimately form amyloid fibrils, we have investigated the consequence of the exposure of murine fibroblasts (NIH-3T3 cells) to prefibrillar aggregates formed from the HypF-N domain and compared the results with findings reported previously with cells exposed to peptides and proteins that are specifically associated with amyloid diseases. This study has enabled us to explore whether the mechanisms by which protein aggregation results in cellular toxicity share a common basis or are protein-specific even in the case of proteins not associated with disease. In particular, we have examined those cellular characteristics found to be perturbed by aggregates of disease-associated proteins, notably the intracellular redox status and the levels of Ca^{2+} ions; we have also investigated the apoptotic or necrotic status of cells following prolonged exposure to the aggregates and explored the reversibility of cell damage occurring prior to cell death. We suggest, on the basis of our findings, that the toxicity of misfolded and aggregated states of different peptides and proteins proceeds through the modification of the same specific biochemical properties in the exposed cells and that such a modification depends on the type of aggregate rather than on the specific amino acid sequence of the aggregated protein. It can therefore be predicted that the cascade of biochemical modifications triggered by the exposure of cells to any aggregated polypeptide chain ultimately leading to cell death, at least in most cases, starts with the alteration of the same cellular parameters.

EXPERIMENTAL PROCEDURES

Reagents—Dichlorodihydrofluorescein diacetate (CM-H_2 DCFA), Fura2-AM, Fluo-3-AM, Texas Red STP ester sodium salt, and wheat germ agglutinin-conjugated fluorescein were from Molecular Probes (Eugene, OR). The caspase 3 assay, cell culture media, materials for microscopy analysis, and other reagents were obtained from Sigma-Aldrich. NIH-3T3 murine fibroblasts were routinely cultured in Dulbecco's modified Eagle's medium (Invitrogen) containing 10% bovine calf serum, unless otherwise stated and 3.0 mM glutamine in a 5% CO_2 humidified environment at 37 °C. 100.0 units/ml penicillin and 100.0 μg/ml streptomycin were added to the media. The cells were used for a maximum of 20 passages. HypF-N was purified as described previously (11). Rabbit anti-HypF-N polyclonal antibodies were provided by Primm S.r.l. (Milan, Italy); Alexa-488-conjugated anti-rabbit IgG secondary antibodies were from Molecular Probes.

Formation and Labeling of Prefibrillar Aggregates—Prefibrillar aggregates of HypF-N were obtained by incubating the protein for 48 h at room temperature at a concentration of 0.3 mg ml^{-1} in 30% (v/v) trifluoroethanol, 50 mM sodium acetate, pH 5.5. The solution was centrifuged, and the resulting pellet was dried under N_2 to remove the remaining solvent, dissolved in RPMI serum-free medium, and immediately added to the culture medium of cells grown on coverslips to a final protein concentration of 20 μM. The presence of HypF-N aggregates inside cells was detected by labeling preformed aggregates with Texas Red as follows. To 1.0 mg of the protein aggregates dissolved in 0.1 ml of 0.1 M sodium bicarbonate buffer, pH 8.5, 10 μl of a 10 mg/ml Texas Red solution in Me_2SO was added slowly. After 1 h at room temperature with continuous stirring, the reaction was stopped by adding 10 μl of 1.5 M hydroxylamine, pH 8.5. The cells were then counterstained with fluorescein-conjugated wheat germ agglutinin (50 μg/ml) for 15 min to detect plasma membrane profiles. Coverslips containing the cells and the labeled prefibrillar aggregates were then mounted on the stage of a confocal Bio-Rad MCR 1024 ES scanning microscope (Bio-Rad) equipped with a krypton/argon laser source (15 mW) for fluorescence measurements. Observations were performed using a Nikon Plan Apo 60× oil immersion objective. Texas Red fluorescence was revealed at 568-nm excitation, and fluorescein was revealed at 488-nm excitation. A series of optical sections (512 × 512 pixels) 1.0 μm in thickness was taken through the cells at intervals of 0.8 μm. 20 optical sections for each examined sample were then projected as single composite image by superimposition. In the indirect immunofluorescence experiments, the cells were plated on glass coverslips and incubated with the prefibrillar aggregates. Then the cells were fixed in 2.0% buffered paraformaldehyde for 10 min at room temperature and blocked with a 0.5% bovine serum albumin and 3.0% glycerol solution in PBS. After washing, the coverslips were incubated with rabbit polyclonal anti-HypF-N antibodies diluted 1:100 in PBS with bovine serum albumin for 60 min. The immunoreaction was revealed with Alexa-488-conjugated anti-rabbit secondary antibodies (Molecular Probes) diluted 1:200. Negative controls were obtained by substituting blocking solution for the primary antibody. Counterstaining for the nuclei was performed with propidium iodide. The fluorescence was analyzed by confocal laser microscopy (Bio-Rad) using two emission lines at 488 and 568 nm for Alexa-488 and propidium iodide excitation, respectively.

Assay of Cellular Toxicity—Aggregate cytotoxicity was assessed by the MTT reduction inhibition assay (20). NIH-3T3 cells were plated on to 96-well plates at a density of 10,000 cells/well in 100 μl of fresh medium. After 24 h, the culture medium was exchanged with 100 μl of RPMI serum-free medium without red phenol. The cells were exposed to the HypF-N aggregates for differing lengths of time as previously reported (12). 10.0 μl of a stock MTT solution in PBS was then added to the cells to a final concentration of 0.5 mg/ml, and the incubation was continued for a further 2 h. At this time, cell lysis buffer (100 μl/well; 20% SDS, 50% *N*,*N*-dimethylformamide, pH 4.7) was added, and the samples were incubated overnight at 37 °C in a humidified incubator. The absorbance of blue formazan was measured at 570 nm using an automatic plate reader as described previously (12). Control experiments were performed by exposing cells to solutions of the nonaggregated, monomeric protein (final concentration, 20.0 μM) for the same lengths of time.

Reversibility of Cell Damage—Reversibility of cell impairment was assessed by performing the MTT assay on cells cultured in serum-free media to avoid cell duplication; the cells were incubated with a serum-free medium containing 20.0 μM of aggregated protein for different lengths of time, washed, and cultured in serum-free medium for 24 h. As a control, the cells were exposed to a serum-free medium containing the same amount of soluble HypF-N. To assess the role of proteasomal involvement, the cells were treated with 10.0 μM lactacystin for varying lengths of time before incubation with a serum-free medium containing 20.0 μM of protein aggregates; at the end of the incubation period, the cells were cultured for 24 h in fresh, serum-free medium and then subjected to the MTT assay. The controls were prepared by incubating cells with lactacystin and then exposing them to 20.0 μM soluble HypF-N for the same lengths of time.

Measurement of the Production of Intracellular Reactive Oxygen Species—Intracellular ROS assays were performed using the ROS-sensitive fluorescent probe CM-H_2 DCFA. NIH-3T3 cells were seeded in 6-well plates at 5 × 10^4 cells/0.8 ml/well. After 24 h, the cells were incubated in the presence of 20.0 μM aggregated protein for differing lengths of time. At the end of the incubation, the cells were washed with PBS and loaded with 5.0 μM CM-H_2 DCFA in the culture medium for 15 min at 37 °C, washed with PBS, and then lysed with RIPA buffer (50 mM Tris-HCl, pH 7.5, 150 mM NaCl, 100 mM NaF, 2.0 mM EGTA, 1.0 mM sodium vanadate, 1% Triton, 10.0 μg/ml aprotinin, 10.0 μg/ml leupeptin). ROS levels were detected in the samples by measuring the fluorescence of the oxidized CM-H_2 DCFA with a PerkinElmer Life Sciences 55 spectrofluorimeter (Wellesley, MA), with excitation and emission wavelengths of 488 and 520 nm, respectively). CM-H_2 DCFA fluorescence into intact cells was also detected using a confocal Bio-Rad MCR 1024 ES scanning microscope equipped with a krypton/argon laser source (15 mW). A series of optical sections (512 × 512 pixels) was taken through the depth of the cells with a thickness of 1.0 μm at intervals of 0.8 μm. Twenty optical sections for each examined sample were then projected as a single composite image by superimposition. The time course analysis of ROS production was performed using the software Time Course Kinetic (Bio-Rad).

Measurements of Intracellular Free Ca^{2+} Levels—The levels of free Ca^{2+} present in the cytosol were measured using the fluorescent probes

Fura2-AM or Fluo-3-AM (21). Subconfluent plates were incubated for differing lengths of time in the presence of a solution containing 20.0 μM of protein aggregates. The cells were washed with PBS and incubated in Dulbecco's modified Eagle's medium supplemented with 10.0% fetal calf serum containing 10.0 μM Fura2-AM. To increase the effectiveness of the probe, Fura2-AM stock solutions (10 mM in dry Me_2SO) were mixed in a 1:1 ratio with 20% pluronic acid F127 prior to addition to the cell medium. Incubation was carried out at 37 °C for 1 h, and then the extracellular dye was removed by washing with a large excess of 10 mM MOPS buffer, pH 7.0, containing 115 mM KCl, 20 mM NaCl, 1.0 mM EGTA, and 1.0 mM $MgCl_2$. The cells were resuspended in 50 μl of the same buffer, counted, and then diluted to a density of 1.0×10^6 cells/ml in a spectrofluorimetric cuvette thermostatted at 25 °C. Intracellular Ca^{2+} concentrations were then calculated using standard protocols (21). In a separate set of experiments intracellular Ca^{2+} was imaged in intact cells using the Ca^{2+}-sensitive probe Fluo-3 and the laser confocal microscope used for intracellular ROS imaging. The cells were cultured on collagen IV-coated glass coverslips, and dye loading was performed by incubating cells with 5.0 μM Fluo-3 for 20 min at 37 °C in the culture medium. Then the coverslips were mounted in a chamber and placed on the stage of the confocal microscope. Fluo-3 fluorescence was monitored at a wavelength of 488 nm by collecting the emitted fluorescence with a Nikon Plan Apo 60× oil immersion objective through a 510-nm-long wave pass filter. The time course analysis of intracellular calcium was performed using the software Time Course Kinetic (Bio-Rad).

Assays for Cell Apoptosis—The extent to which the apoptotic pathway had been triggered in 80% confluent cells exposed for 48 h to a 20 μM final concentration of HypF-N aggregates was determined by measuring caspase-3 activation using a colorimetric 96-well plate assay system (Sigma) as specified by the provider.

RESULTS

An important question in the investigation of protein aggregate toxicity is to assess whether the effects of aggregates to cells follow aggregate internalization. We first investigated whether the prefibrillar aggregates of HypF-N added to the cell culture medium appeared in the cytoplasm, by labeling the aggregates with the fluorescent probe Texas Red. Fig. 1 shows confocal microscopy images at different focal lengths of cells exposed for 3 h to the labeled HypF-N aggregates; similar images were seen after 1 h of exposure (not shown). The aggregated species can be seen to have accumulated in the vicinity of the plasma membrane (Fig. 1*A*) and also to be present in the intracellular focal plane (Fig. 1*B*, *arrows*). The ingress of the aggregates into the cells does not result simply from the enhanced hydrophobicity of the aggregate-Texas Red complex, because similar data were obtained using unlabeled aggregates whose presence inside cells was detected by immunofluorescence using polyclonal anti-HypF-N antibodies (Fig. 1*C*). This result shows that early aggregates of HypF-N added to the cell culture medium are able to be internalized, although the mechanism of aggregate translocation inside cells requires further investigation.

The biochemical parameters we investigated in the cells exposed to the prefibrillar aggregates were the redox status and the intracellular free Ca^{2+}. Fig. 2 shows the results of the experiments aimed at determining the levels of ROS that are generated within cells following exposure for 3 h to 20 μM HypF-N in both soluble and aggregated forms. A significant increase in ROS, concomitant with a decrease in cell viability as detected by the MTT assay, was found (Fig. 2*A*). ROS increase and cytotoxicity, however, were not present in cells incubated, prior to exposure to the aggregates, in the presence of 0.10 mM α-tocopherol (vitamin E), a lipid-soluble antioxidant that is very effective in suppressing membrane lipid peroxidation (Fig. 2*A*). Similar results were obtained using propylgallate or promethazine as reducing agents (data not shown). The ROS levels after exposure to HypF-N aggregates were also determined by monitoring cells with confocal microscopy in the presence of the fluorescent probe CM-H_2 DCFA. As in the experiments performed using cell lysates, a considerable increase in ROS levels was found in living cells exposed to the aggregates, whereas no ROS increase was observed when the same cells were treated with 0.10 mM α-tocopherol (Fig. 2*B*). These findings show that the HypF-N prefibrillar aggregates modify the redox status of cells in a manner closely similar to that previously reported for peptides and proteins that are associated with protein deposition diseases (see "Discussion").

To assess whether the HypF-N aggregates induced an increase of intracellular Ca^{2+} levels, cell media were supplemented with a 1:1 mixture of 10.0 μM Fura2-AM, 20% pluronic acid F127 (see "Experimental Procedures"). Fig. 3*A* shows that intracellular Ca^{2+} levels rise by a factor of about 2 in cells exposed for 3 h to a 20 μM solution of aggregated protein compared with control experiments where cells were incubated in the presence of the same quantity of soluble HypF-N. This increase, along with a concomitant decrease in cell viability, as determined by the MTT test, was abolished when the cells were cultured in a Ca^{2+}-free medium (Fig. 3*A*). The intracellular Ca^{2+} levels after exposure to the HypF-N aggregates were also monitored *in vivo* by confocal microscopy (see "Experimental Procedures"). A considerable increase in Ca^{2+} was found in cells exposed to the aggregates, whereas no increase was observed when cells were cultured in a Ca^{2+}-free medium (Fig. 3*B*). These data reveal that intracellular Ca^{2+} levels are modified in the cells exposed to the HypF-N aggregates in a manner similar to that reported previously for cells incubated in the presence of disease-associated peptides and proteins including the Aβ peptide, human islet amylin, the amyloidogenic prion protein fragment, and Cu,Zn-SOD (see "Discussion").

Intracellular Ca^{2+} and ROS levels were also monitored by confocal microscopy in cells incubated in the presence of α-tocopherol prior to exposure to the HypF-N aggregates and in cells cultured in Ca^{2+}-free medium during the time they were exposed to the aggregates, respectively. Fig. 4 shows that the ROS levels are high following exposure to aggregates even in the absence of Ca^{2+} in the medium. By contrast, free Ca^{2+} levels in cells pretreated with α-tocopherol before exposure to HypF-N aggregates were considerably lower than in cells not treated with α-tocopherol and the same as in control cells exposed to the protein in its soluble form.

The substantial increase in ROS caused by the HypF-N aggregates even in the absence of Ca^{2+} in the medium indicates that oxidative stress is, at least in part, independent of the rise of the intracellular Ca^{2+} levels. This conclusion is supported by the observed time courses of both Ca^{2+} and ROS increases, where the ROS increase is found to precede the Ca^{2+} rise during the first 20 min of exposure to the aggregates (Fig. 5). However, both events occur rapidly compared with other changes in cellular functions such as apoptosis or necrosis, being almost complete after 60 min of exposure. The finding that the viability of cells cultured in Ca^{2+}-free medium is unaffected by exposure to the HypF-N aggregates, although displaying enhanced ROS production, indicates that, at least under our conditions, oxidative stress does not by itself generate cytotoxicity.

We have also investigated the degree of reversibility of the rise of both intracellular ROS and Ca^{2+} levels, along with the associated cell damage. The effect of preincubation of cells in the presence of lactacystin (10.0 μg/ml), a potent proteasome inhibitor, before exposure to the aggregates was also examined. Cells were cultured in serum-free medium to avoid cell division following transfer in aggregate-free fresh medium. Fig. 6 shows that cell damage appears to be almost completely reversible after exposure to the aggregates for relatively short lengths of time (less than 5 h) when the cells almost completely recover the ability to reduce MTT. For longer times of exposure (until 15 h)

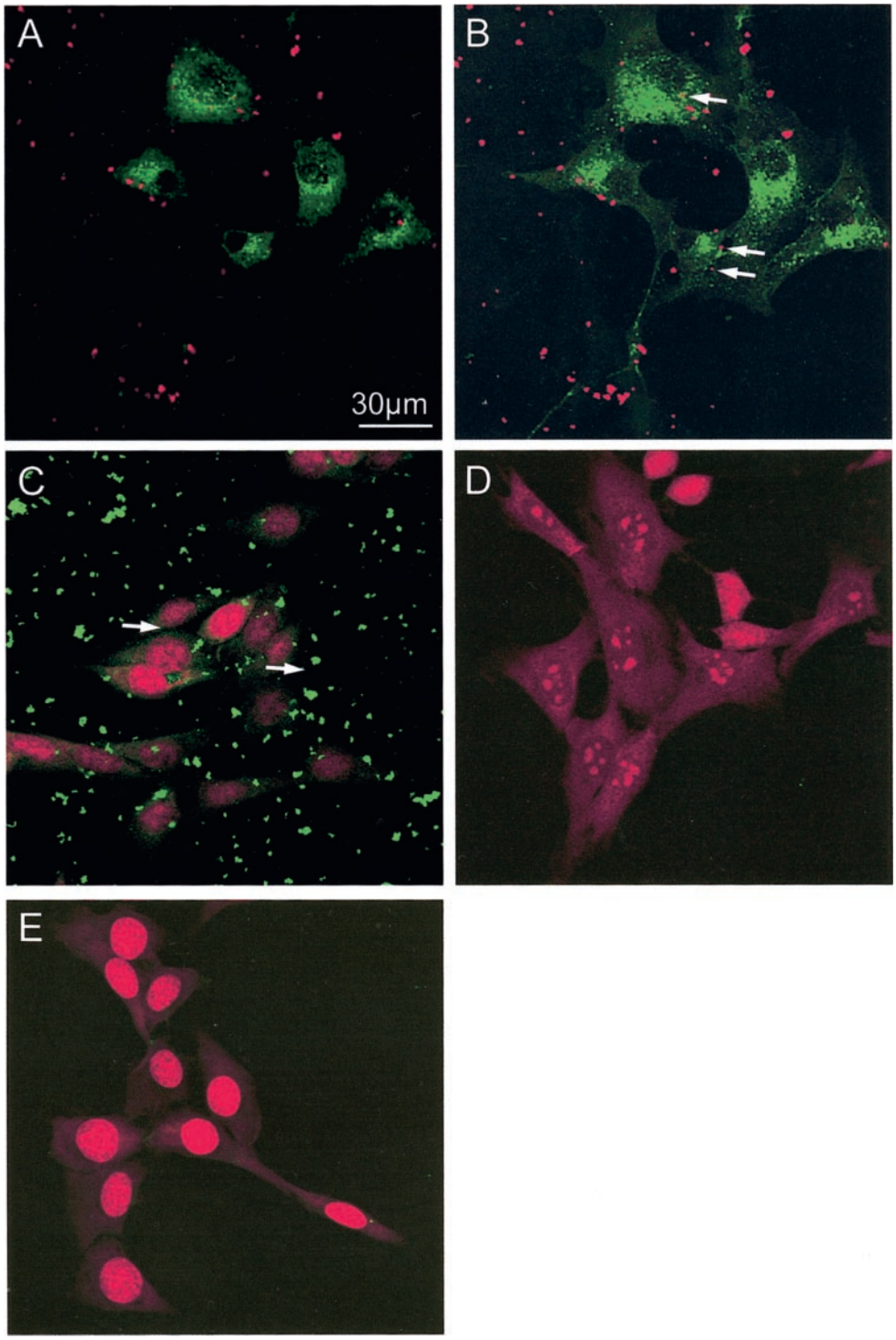

FIG. 1. **Early HypF-N aggregates penetrate into cells.** Confocal microscopy images showing aggregates in contact with, and penetrating into, the plasma membrane and cytoplasm of cells. The cells were incubated for 3 h in the presence of the aggregates previously labeled with Texas Red and added to the cell culture medium (see "Experimental Procedures"). Counterstaining was performed with fluorescein-conjugated wheat germ agglutinin to detect plasma membrane profile (*green*). *A*, top focal length; aggregates in the culture medium and in contact with the plasma membrane. *B*, middle focal length of the same field; *arrowheads* indicate aggregates within the cell. *C*, immunofluorescence detection of the HypF-N aggregates into cells. The aggregates were detected with anti-HypF-N antibodies and Alexa-488-labeled secondary antibodies as specified under "Experimental Procedures." A diffuse intracellular green fluorescence is evident. Counterstaining for the nuclei was performed with propidium iodide (*red*). *D*, control cells treated with soluble HypF-N and incubated with primary and secondary antibody. *E*, negative control. The cells were incubated with aggregates and then only with secondary antibody without primary antibody.

cells recovered viability only partially. Moreover, the cells stressed upon pretreatment with lactacystin followed by exposure to the aggregates were more susceptible to damage than were untreated cells; in this case, the reversal of the toxic effects was dependent upon the length of the time of preincubation with lactacystin. After 15 h of preincubation, the cell damage was not reversed when the cells were moved to fresh media, whereas for 5 and 3 h of preincubation, reversal was partial or complete, respectively, indicating a different degree of impairment of the mechanisms of clearance of the aggregates.

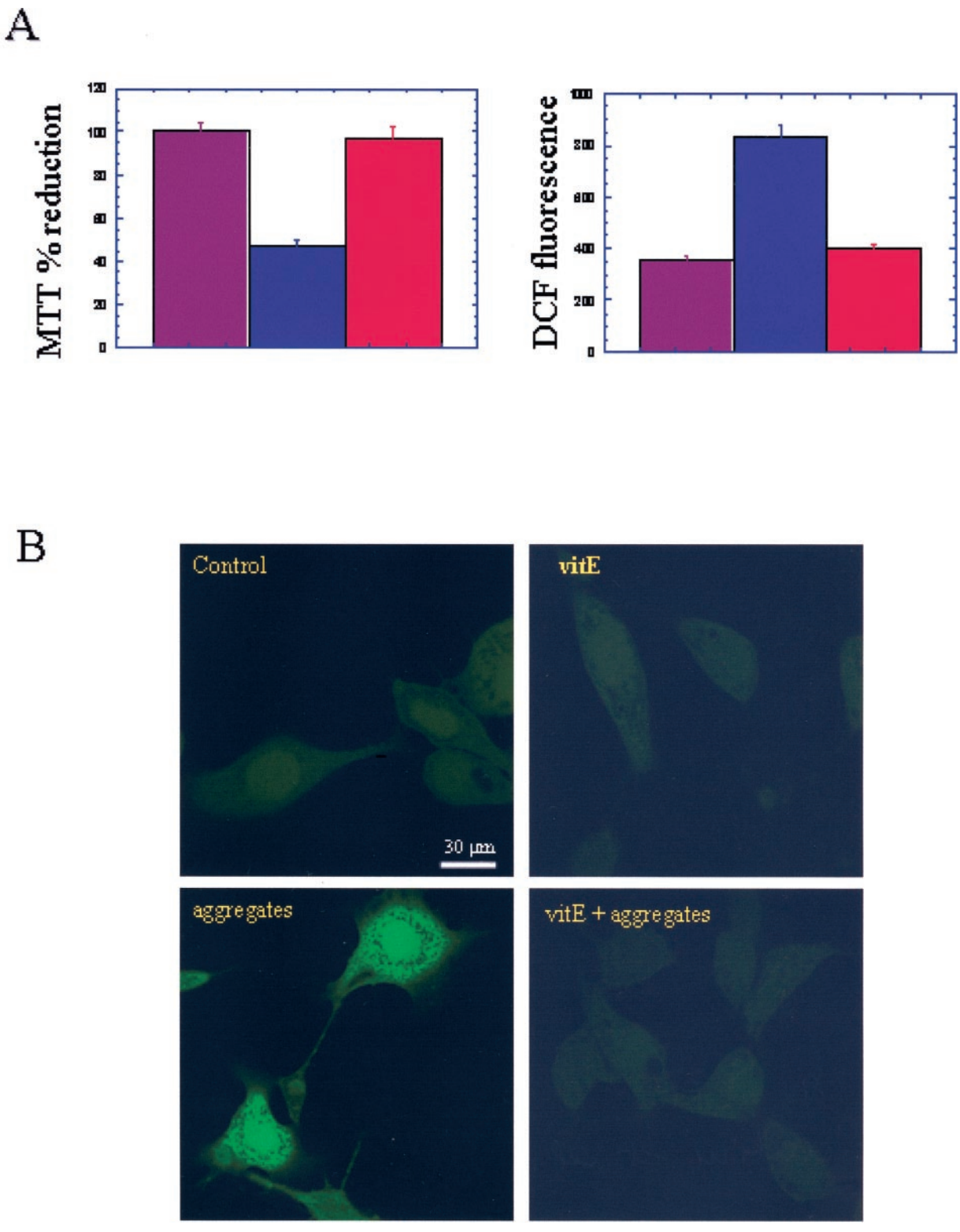

FIG. 2. **Redox status and viability of NIH-3T3 cells exposed to soluble and aggregated HypF-N.** *A*, cells were exposed for 3 h to 20 μM solutions of soluble HypF-N (*control*, *left bar*), aggregated HypF-N, (*middle bar*), and aggregated HypF-N after exposure to α-tocopherol (*vitE*, *right bar*), and then lysed to measure the amount of generated ROS (*right panel*) (see "Experimental Procedures" for details). Cell viability (*left panel*) was measured by the MTT test. The values shown are the averages of five experiments carried out in triplicate. *B*, confocal microscopy imaging of the redox status of cells exposed to 20 μM soluble HypF-N (*top left panel*), 20 μM soluble HypF-N after exposure to 0.10 mM α-tocopherol (*vitE*) (*top right panel*), 20 μM aggregated HypF-N (*bottom left panel*) and 20 μM aggregated HypF-N after exposure to 0.10 mM α-tocopherol (*vitE*) (*bottom right panel*). ROS production was revealed by incubating for 10 min the exposed cells in the presence of the redox fluorescent probe CM-H_2 DCFA (see "Experimental Procedures" for details).

It has previously been reported that, after prolonged exposure to the HypF-N aggregates, cells undergo death, as shown by the trypan blue exclusion assay (12). We have not investigated in detail the features of cell death under our conditions; however, we found a necrotic rather than an apoptotic condition in our cells exposed for 24 h to the aggregates (data not

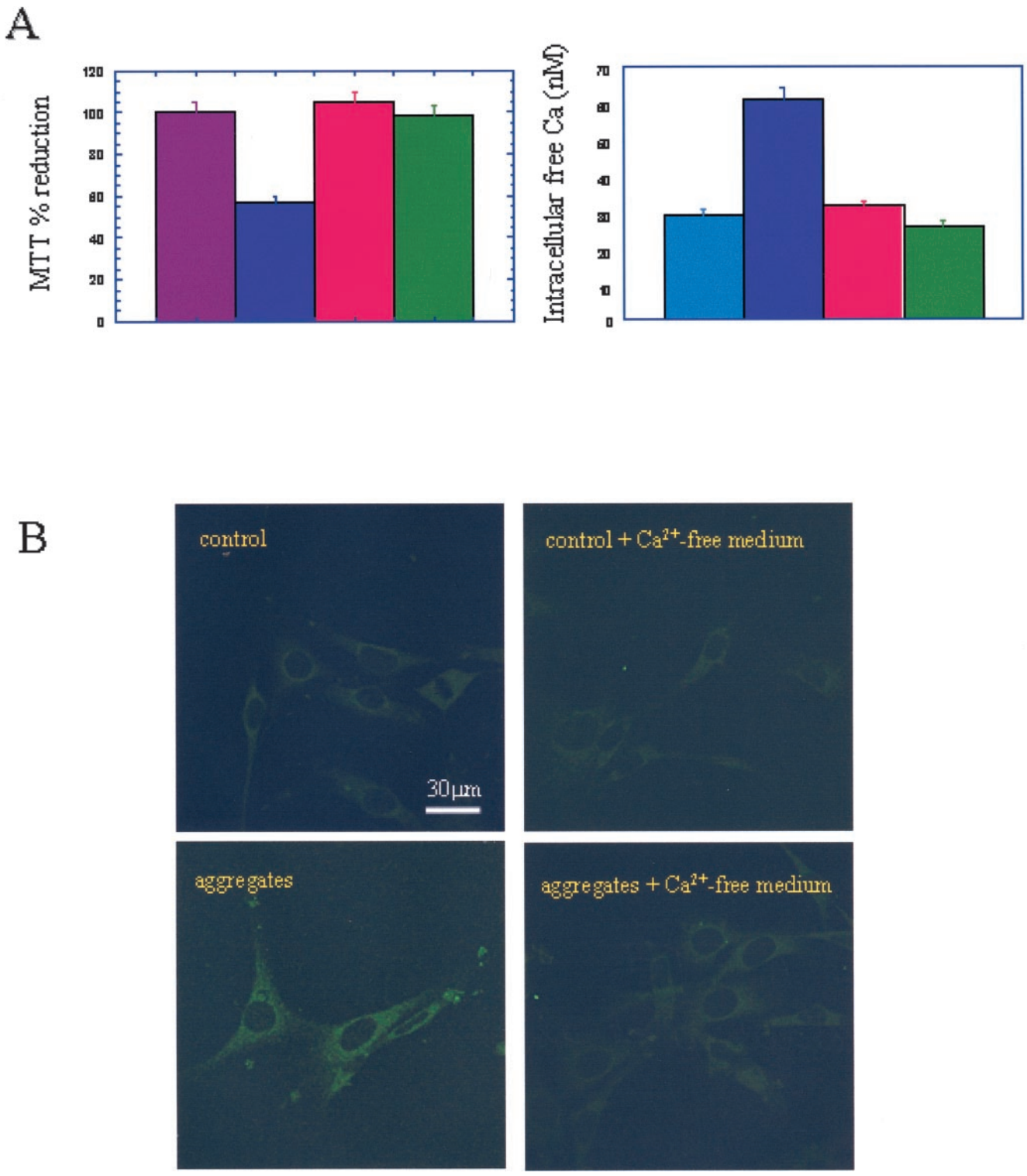

FIG. 3. **Intracellular free Ca^{2+} levels and viability of cells exposed to soluble or aggregated HypF-N.** *A*, cells were exposed for 3 h to solutions of 20 μM soluble HypF-N (*first bar*), 20 μM aggregated HypF-N (*second bar*), 20 μM soluble HypF-N in the presence of Ca^{2+}-free medium (*third bar*), and 20 μM aggregated HypF-N in the presence of Ca^{2+}-free medium (*fourth bar*). The cells were then lysed to measure the amount of Ca^{2+} using the fluorescent probe Fura2-AM (*right panel*) (see "Experimental Procedures " for details). Cell viability was measured by the MTT test (*left panel*). The values shown are the averages of five experiments carried out in triplicate. *B*, confocal microscopy imaging of the intracellular free Ca^{2+} levels of cells exposed to 20 μM soluble HypF-N (*top left panel*), 20 μM soluble HypF-N in the presence of Ca^{2+}-free medium (*top right panel*), 20 μM aggregated HypF-N (*bottom left panel*), and 20 μM aggregated HypF-N in the presence of Ca^{2+}-free medium (*bottom right panel*). Intracellular Ca^{2+} was revealed by incubating the exposed cells for 15 min in the presence of the fluorescent dye Fluo-3 (see "Experimental Procedures" for details).

shown). Nevertheless, a progressive caspase-3 activation was initially present, reaching a maximum (around 250%) after 6–7 h of exposure to the aggregates, indicative of an apoptotic response (data not shown). Although preliminary, these data suggest that, in our exposed cells, the apoptotic pathway is initially triggered but is not sustained and is followed by ne-

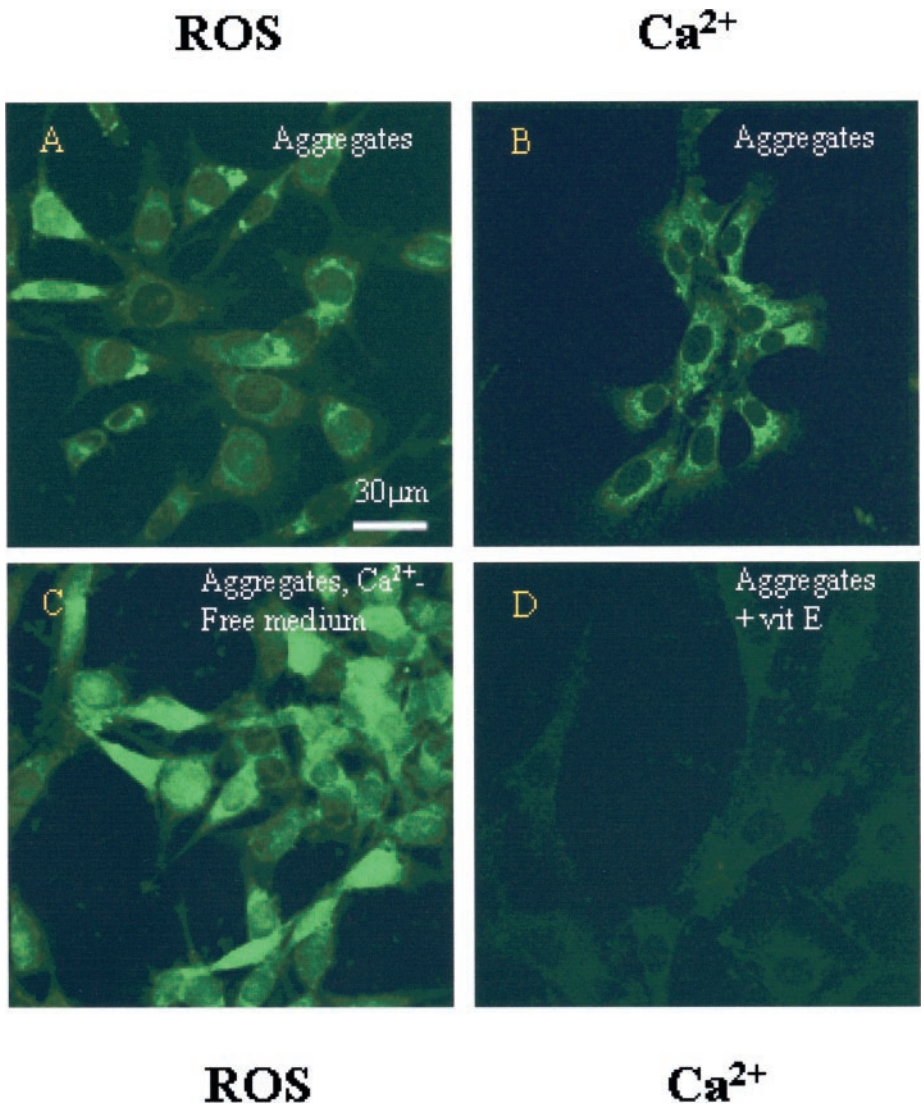

FIG. 4. **ROS and Ca^{2+} levels in cells exposed to HypF-N aggregates.** ROS and intracellular free Ca^{2+} levels were imaged by confocal microscopy using the fluorescent dyes CM-H_2 DCFA (*left panels*) and Fluo-3 (*right panels*), respectively, as probes according to the procedures described in the captions to Figs. 2 and 3 and under "Experimental Procedures." *A* and *C*, cells were exposed to 20 μM aggregated HypF-N (*A*) or to 20 μM aggregated HypF-N in the presence of Ca^{2+}-free medium (*C*) and checked for ROS levels. *B* and *D*, cells were exposed to 20 μM aggregated HypF-N (*B*) or to 20 μM aggregated HypF-N after preincubation with 0.10 mM α-tocopherol (*VitE*) (*D*) and checked for free Ca^{2+} levels. Twenty optical sections for each examined sample were then projected as a single composite image by superimposition.

crotic death. A deeper investigation of the biochemical features of cell death following exposure to the toxic aggregates is presently underway.

DISCUSSION

It is now well established that the aggregation process of peptides and proteins leading to the appearance of amyloid fibrils involves a series of relatively well defined steps. The protein aggregates studied here consist largely of a mixture of globules around 2.5 nm in diameter, other aggregates with variable widths not exceeding 8.0 nm, chains formed by several of these globules, and rare "doughnuts" with a central pore (12, 22). Similar species have previously been imaged for a number of peptides and proteins associated with amyloid disease (16, 23–27). We have not investigated in detail the features of the membrane translocation leading the HypF-N prefibrillar assemblies to appear inside the cells as shown in Fig. 1; however, our findings agree with similar data concerning prefibrillar aggregates of poly(Q), CspB-1, and human endostatin (27, 28).

It is increasingly recognized that the disruption of the integrity of cell membranes by misfolded peptides and proteins as well as pore-forming proteins is a primary step in the induction of cell death (25, 29–31). Cell death can then occur as a consequence of either the imbalance of ion homeostasis and transmembrane electrochemical gradients or the impairment of the various signaling pathways, suggesting that this is the primary origin of cell damage and death that results from the exposure of cells to the HypF-N aggregates.

A large body of data has recently been reported indicating that cells exposed to amyloid aggregates in most cases display remarkable increases in intracellular ROS and free Ca^{2+} (32–38). However, the relationship between Ca^{2+} and ROS increases as well as the biochemical modifications underlying them have not been fully explained.

In general, it is not clear why the formation of amyloid fibrils or their precursors triggers ROS production and free Ca^{2+} increase. Varying hypotheses have been put forward, including an increase of the oxidative metabolism to clear the excess of free Ca^{2+} (39), the impairment of the functionality of the endoplasmic reticulum and mitochondria affecting Ca^{2+} levels and ROS production (reviewed in Refs. 31 and 40) or an involvement of metal ions (41). The increase in free Ca^{2+} has also been attributed to the formation of nonspecific ion channels in

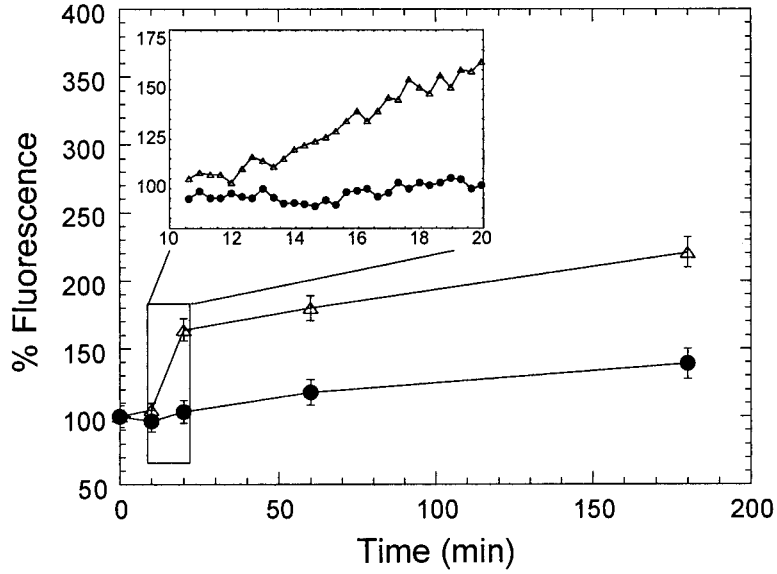

FIG. 5. **Time courses of the changes in the ROS and free Ca^{2+} levels in cells following exposure to the HypF-N aggregates.** The data were obtained by measuring the fluorescence of CM-H_2 DCFA (ROS, △) and Fura2-AM (free Ca^{2+}, ●) in the presence of lysates of cells exposed to HypF-N aggregates. The experimental details are given under "Experimental Procedures." The data represent the means ± S.D. of three independent experiments. The *inset* shows the initial changes in the same parameters during the first 20 min of cell exposure to HypF-N aggregates (the *boxed area* of the larger graph), as determined by continuous measurements of fluorescence in the field of the confocal microscope upon the addition of the fluorescent probes CM-H_2 DCFA and Fluo-3. The fluorescence values are reported as percentages of the values determined at time 0.

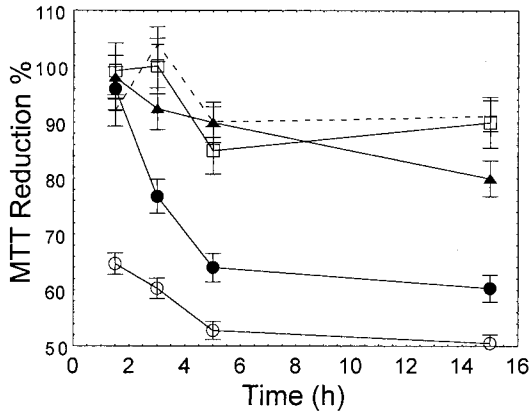

FIG. 6. **Reversibility of cytotoxicity promoted by HypF-N aggregates.** *Black circle*, cytotoxicity in cells exposed to serum-free medium containing the aggregates (20 μM) for 1, 3, 5, and 15 h. The values are expressed as percentages with respect to the values found in control cells exposed to 20 μM of soluble HypF-N in serum-free medium. *Dotted line*, cytotoxicity in cells cultured for 24 h in a fresh, serum-free and aggregate-free medium following exposure to the HypF-N aggregates (20 μM) in serum-free medium for the indicated times relative to cell exposed to serum-free medium containing the same amount of soluble HypF-N washed and cultured in a fresh serum-free medium for 24 h. Cytotoxicity in cells preincubated for 3 h (*open square*), 5 h (*black triangle*), and 15 h (*open rhomboid*), in the presence of 10 μg/ml of lactacystin, exposed for 1 h, 3 h, 5, and 15 h to the HypF-N aggregates (20 μM) in serum-free medium and then cultured in fresh, serum-free and aggregate-free medium for 24 h. Cell damage was evaluated by the MTT test (see "Experimental Procedures"). The values are expressed as percentages with respect to the values found in control cells exposed to 20 μM of soluble HypF-N in serum-free medium for corresponding lengths of time and then cultured in fresh, serum-free medium for 24 h. The experiments with lactacystin were carried out as indicated under "Experimental Procedures."

the membranes of cells exposed to protofibrils of varying disease-associated peptides and proteins (23, 24, 26, 42–44).

Under our experimental conditions, we have found a significant increase in ROS and free Ca^{2+} in cells exposed to HypF-N prefibrillar aggregates, in agreement with data previously reported for aggregates of a number of peptides and proteins associated with amyloid diseases (32–38). Our findings support recently reported data (18) suggesting that cell damage results from common features of the aggregated states of different (possibly most) proteins rather than from specific properties of particular sequences.

We have not investigated the origin of the increase in ROS and in free Ca^{2+} in cells exposed to the HypF-N aggregates; however, under our conditions, ROS and free Ca^{2+} increases appear to be early modifications. Furthermore, ROS increase appears to precede the rise of free Ca^{2+} and is found even in the absence of the latter but does not appear to be sufficient by itself to impair cell viability, at least for the times we have investigated. Oxidative stress without impairment of cell viability or proteasome activity has recently been reported in other systems (45, 46). Recent atomic force microscopy images show that solutions of early (24–48 h) prefibrillar aggregates of HypF-N contain only rare doughnut-shaped assemblies but are able to permeabilize reconstituted lipid vesicles (22); therefore, the increased presence of these structures at the surface of biological membranes inducing membrane permeabilization and Ca^{2+} entry cannot be excluded.

The data reported support the possibility that, under our conditions, ROS increase in cells exposed to the aggregates can be the consequence of the activation of the oxidative metabolism providing the membrane pumps with the ATP needed to clear the free Ca^{2+}, and possibly other ions, entering the cytosol from the extracellular medium and/or the intracellular stores (39). For short times of exposure, the Ca^{2+} could be efficiently pumped out, thus maintaining normal cytosolic levels, as supported by the early time courses of ROS and free Ca^{2+} increases in cells in the presence of aggregates, where the former precedes the latter. The subsequent free Ca^{2+} increase could be the consequence of the oxidative impairment of both the Ca^{2+}-ATPases and calmodulin, whose oxidized form is, in itself, unable to activate the Ca^{2+} pump (reviewed in Ref. 39) and of the activation of caspases by the Ca^{2+} excess (reviewed in Ref. 31). Indeed, we have not assayed the Ca^{2+}-ATPase activity in our cells exposed to the aggregates for short lengths of time (5–7 h), but we have found in them a significant increase of the activity of caspase 3 (not shown). ROS and free Ca^{2+} levels do not increase in cells previously incubated with reducing agents, where oxidative metabolism and the activity of ion pumps are likely to be maintained. However, our data indicate that ROS increase is not determined by the ingress into the cells of the sole extracellular Ca^{2+} because a rise of ROS was found even in cells cultured in Ca^{2+}-free media following exposure to the aggregates.

An issue of great importance for understanding the origins of cytotoxicity of protein aggregates and indeed for the development of therapeutic strategies against amyloid disease is the possibility that protein aggregation and the resulting cell dam-

age can be reversed and the amyloid deposits cleared when the conditions that favor aggregation are eliminated. Indeed, there is evidence for clearance of aggregates in animal models (47); in addition, treatments that reduce the supply of fibril precursor proteins, such as liver transplantation, can induce a regression of amyloid deposits in human amyloidoses (48, 49). Our findings that cells exposed to HypF-N aggregates for short lengths of time show impaired viability but recover when they are moved to fresh, aggregate-free media indicate that cell damage is fully reversible provided the time of exposure to the aggregates is short. The cells preincubated with lactacystin and then exposed to HypF-N aggregates show greater impairment of function and lower degrees of reversibility depending on the time of preincubation and hence on the extent of impairment of the proteasomal activity. This result is consistent with recent observations that malfunctioning of the ubiquitin-proteasome pathway occurs in a number of neurodegenerative diseases (45, 46, 50–52). Reversal of cell damage has also been reported in cultured chondrocytes containing protein aggregates in the endoplasmic reticulum (53) and in mice expressing a mutated huntingtin fragment (47). These results, taken together, indicate that the impairment of viability in cells exposed to the aggregates is a progressive phenomenon that becomes more damaging under conditions where the cellular clearance mechanisms are hindered.

It is generally believed that the origins of cell death associated with protein aggregates is a result of the stimulation of the apoptotic response, although recent data show a necrotic rather than an apoptotic death in some cases (54–57). Although the biochemical features of cell death following exposure to the toxic HypF-N aggregates are currently under investigation, our preliminary results support these suggestions. In fact, despite a progressive increase of the caspase 3 activity reaching a maximum in cells after 6–7 h of exposure to the HypF-N aggregates, necrosis appears to be the dominant feature of cell death, at least under the same conditions as those used here.

Our data on the early increase of intracellular free Ca^{2+} and ROS and on the initial activation of the apoptotic machinery followed by secondary necrosis are in agreement with a recent study indicating that caspases, and particularly caspase-3, may cleave and inactivate the plasma membrane Ca^{2+} pumps (58). It has been proposed that the loss of function of the latter during apoptosis results in Ca^{2+} overload and slowing down of apoptosis followed by secondary cell lysis or necrosis (reviewed in Ref. 31).

The data on the aggregability of most proteins under suitable conditions, such as those found in aged organisms, on the generic toxicity of protein aggregates and its common biochemical features support the hypothesis that the appearance in cells of such species may be a rather frequent event causing subtle impairments of cell viability even in the absence of an evident amyloid phenotype. If this were to be the case, other pathological conditions in addition to those that are currently recognized to be linked to protein aggregation could be associated with the intracellular or extracellular deposition of misfolded proteins or their early aggregates. Indeed, an increasing number of reports indicate that many common or rare degenerative diseases are associated with misfolding and deposition of previously unsuspected proteins (reviewed in Ref. 6).

REFERENCES

1. Thomas, T., Thomas, G., McLendon, C., Sutton, T., and Mullan, M. (1996) *Nature* **380,** 168–171
2. Pepys, M. B. (1995) in *Oxford Textbook of Medicine* (Wheaterall, D. J., Ledingham, J. G., and Warrel, D. A., eds) 3rd Ed., pp 1512–1524, Oxford University Press, Oxford
3. Koo, E. H., Lansbury, P. T., and Kelly, J. K. (1999) *Proc. Natl. Acad. Sci. U. S. A.* **96,** 9989–9990
4. Kelly, J. (1998) *Curr. Opin. Struct. Biol.* **8,** 101–106
5. Selkoe, D. J. (2001) *Physiol. Rev.* **81,** 741–766
6. Stefani, M., and Dobson, C. M. (2003) *J. Mol. Med.* **81,** 678–699
7. Chiti, F., Webster, P., Taddei, N., Clark, A., Stefani, M., Ramponi, G., and Dobson, C. M. (1999) *Proc. Natl. Acad. Sci. U. S. A.* **96,** 3590–3594
8. Dobson, C. M. (2001) *Philos. Trans. R. Soc. Lond. B Biol. Sci.* **356,** 133–145
9. Dobson, C. M. (2002) *Nature* **418,** 729–730
10. Gujiarro, J. I. Sunde, M., Jones, J. A., Campbell, I. D., and Dobson, C. M. (1998) *Proc. Natl. Acad. Sci. U. S. A.* **95,** 4224–4228
11. Chiti, F., Bucciantini, M., Capanni, C., Taddei, N., Dobson, C. M., and Stefani, M. (2001) *Protein Sci.* **10,** 2541–2547
12. Bucciantini, M., Giannoni, E., Chiti, F., Baroni, F., Formigli, L., Zurdo, J., Taddei, N., Ramponi, G., Dobson, C. M., and Stefani, M. (2002) *Nature* **416,** 507–511
13. Conway, K. A., Lee, S.-J., Rochet, J. C., Ding, T. T., Williamson, R. E., and Lansbury, P. T. (2000) *Proc. Natl. Acad. Sci. U. S. A.* **97,** 571–576
14. Bhatia, R., Lin, H., and Lal, R. (2000) *FASEB J.* **14,** 1233–1243
15. Goldberg, M. S., and Lansbury, P. T. (2000) *Nat. Cell Biol.* **2,** E115–E119
16. Sousa, M. M., Cardoso, I., Fernandes, R., Guimaraes, A., and Saraiva, M. J. (2001) *Am. J. Pathol.* **159,** 1993–2000
17. Walsh, D. M., Klyubin, I., Fadeeva, J. V., Cullen, W. K., Anwyl, R., Wolfe, M. S., Rowan, M. J., and Selkoe, D. J. (2002) *Nature* **416,** 535–539
18. Kayed, R., Head, E., Thompson, J. L., McIntire, T. M., Milton, S. C., Cotman, C. W., and Glabe, C. G. (2003) *Science* **300,** 486–489
19. Svanborg, C., Agerstam, H., Aronson, A., Bjerkvig, R., Duringer, C., Fischer, W., Gustafsson, L., Hallgren, O., Leijonhuvud, I., Linse, S., Mossberg, A.-K., Nilsson, H., Pettersson, J., and Svensson, M. (2003) *Adv. Cancer Res.* **88,** 1–29
20. Abe, K., and Kimura, H. (1996) *J. Neurochem.* **67,** 2074–2078
21. Grynkiewicz, G., Poenie, M., and Tsien, R. Y. (1985) *J. Biol. Chem.* **260,** 3440–3450
22. Relini, A., Canale, C., Torrassa, S., Rolandi, R., Ghiozzi, A., Rosano, C., Bolognesi, M., Plakoutsi, G., Bucciantini, M., Chiti, F., and Stefani, M. (2004) *J. Mol. Biol.* **338,** 943–957
23. Hirakura, Y., and Kagan, B. L. (2001) *Amyloid* **8,** 94–100
24. Lin, H., Bhatia, R., and Lal, R. (2001) *FASEB J.* **15,** 2433–2444
25. Lashuel, H.A., Hartley, D., Petre, B.M., Walz, T., and Lansbury, P.T. (2002) *Nature* **418,** 291
26. Wang, L., Lashuel, H. A., Walz, T., and Colòn, W. (2002) *Proc. Natl. Acad. Sci. U. S. A.* **99,** 15947–15952
27. Kranenburg, O., Kroon-Batenburg, L. M. J., Reijerkerk, A., Wu, Y.-P., Voest, E. E., and Gebbink, M. F. B. G. (2003) *FEBS Lett.* **539,** 149–155
28. Yang, W., Dunlap, J. R., Andrews, R. B., and Wetzel, R. (2002) *Hum. Mol. Genet.* **11,** 2905–2917
29. Morgan, B. P. (1999) *Crit. Rev. Immunol.* **19,** 173–198
30. Tweten, R. K., Parker, M. W., and Johnson, A. E. (2001) in *Pore Forming Toxins* (van der Goot, G., ed) pp. 15–23, Springer-Verlag, Heidelberg.
31. Orrenius, S., Zhovotovsky, B., and Nicotera, P. (2003) *Nat. Rev.* **4,** 552–565
32. Mattson, M. P. (1999) *Methods Enzymol.* **309,** 733–768
33. Kruman, I. I., Pedersen, W. A., Springer, J. E., and Mattson, M. P. (1999) *Exp. Neurol.* **160,** 28–39
34. Kawahara, M., Kuroda, Y., Arispe, N., and Rojas, E. (2000) *J. Biol. Chem.* **275,** 14077–14083
35. Kanski, J., Varadarajan, S., Aksenova, M., and Butterfield, D. A. (2001) *Biochim. Biophys. Acta* **1586,** 190–198
36. Milhavet, O., and Lehmann, S. (2002) *Brain Res. Rev.* **38,** 328–339
37. Junn, E., and Mouradian, M.M. (2002) *Neurosci. Lett.* **320,** 146–150
38. Wyttenbach, A., Sauvageot, O., Carmichael, J., Diaz-Latoud, C., Arrigo, A.-P., and Rubinsztein, D. C. (2002) *Hum. Mol. Genet.* **11,** 1137–1151
39. Squier, T. C. (2001) *Exp. Gerontol.* **36,** 1539–1550
40. Mattson, M. P., and Liu, D. (2002) *Neuromol. Med.* **2,** 215–231
41. Tabner, B. J., Turnbull, S., El-Agnaf, O. M. A., and Allsop, D. (2002) *Free Radic. Biol. Med.* **32,** 1076–1083
42. Andersson, K., Olofsson, A., Nielsen, E. H., Svehag, S. E., and Lundgreen, E. (2002) *Biochem. Biophys. Res. Commun.* **294,** 309–314
43. Volles, M. J., and Lansbury, P. T. (2002) *Biochemistry* **41,** 4595–4602
44. Kourie, J.I., and Henry, C.L. (2002) *Clin. Exp. Pharmacol. Physiol.* **29,** 741–753
45. Hyun, D.-H., Lee, M., Hattori, N., Kubo, S.-I., Mizuno, Y., Halliwell, B., and Jenner, P. (2002) *J. Biol. Chem.* **277,** 28572–28577
46. Keller, J. N., Huang, F. F., and Markesbery, W. R. (2002) *Neuroscience* **98,** 149–156
47. Yamamoto, A., Lucas, J. J., and Hen, R. (2000) *Cell* **101,** 57–66
48. Gillmore, J. D., Hawkins, P. N., and Pepys, M. B. (1997) *British J. Haematol.* **99,** 245–256
49. Gillmore, J. D., Lovat, L. B., Persey, M. R., Pepys, M. B., and Hawkins P.N. (2001) *Lancet* **358,** 24–29
50. Keller, J. N., Hanni, K. B., and Markesbery, W. R. (2000) *J. Neurochem.* **75,** 436–439
51. McNaught, K. S., and Jenner, P. (2001) *Neurosci. Lett.* **297,** 191–194
52. Waelter, S., Boeddrich, A., Lurz, R., Scherzinger, E., Lueder, G., Lehrach, H., and Wanker, E. E. (2001) *Mol. Biol. Cell* **12,** 1393–1407
53. Pacifici, M., and Iozzo, R. V. (1988) *J. Biol. Chem.* **263,** 2483–2492
54. Velez-Pardo, C., Arroyave, S. T., Lopera, F., Castano, A. D., and Jimenez Del Rio, M. (2001) *J. Alzheimer's Dis.* **3,** 409–415
55. Turmaine, M., Raza, A. Mahal, A. Mangiarini, L., Bates, G. P., and Davies. S. W. (2000) *Proc. Natl. Acad. Sci. U. S. A.* **97,** 8093–8097
56. Lane, N. J., Balbo, A., Fukuyama, R., Rapoport, S. I., and Galdzick, Z. (1998) *J. Neurocytol.* **27,** 707–718
57. Watt, J. A., Pike, C. J., Walencewicz-Wasserman, A. J., and Cotman, C. W. (1994) *Brain Res.* **661,** 147–156
58. Schwab, B. L., Guerini, D., Didszun, C., Bano, D., Ferrando-May, E., Fava, E., Tam, J., Xu, D., Xanthoudakis, S., Nicholson, D. W., Carafoli, E., and Nicotera, P. (2002) *Cell Death Differ.* **9,** 818–831

Prefibrillar Amyloid Protein Aggregates Share Common Features of Cytotoxicity

Monica Bucciantini, Giulia Calloni, Fabrizio Chiti, Lucia Formigli, Daniele Nosi, Christopher M. Dobson and Massimo Stefani

J. Biol. Chem. 2004, 279:31374-31382.
doi: 10.1074/jbc.M400348200 originally published online May 6, 2004
